

# Detectability of Plasma-Derived Circulating Tumor DNA Panel in Patients Undergoing Primary Treatment for Uveal Melanoma

Jasmine H. Francis,<sup>1,2</sup> Christopher A. Barker,<sup>3</sup> A. Rose Brannon,<sup>4</sup> Julia Canestraro,<sup>1</sup> Melissa Robbins,<sup>1</sup> Christina E. Swartzwelder,<sup>5</sup> Sara Levine,<sup>1</sup> Crystal Law,<sup>1</sup> Michael F. Berger,<sup>4</sup> Alexander Shoushtari,<sup>6,7</sup> and David H. Abramson<sup>1,2</sup>

<sup>1</sup>Department of Surgery (Ophthalmic Oncology Service), Memorial Sloan Kettering Cancer Center, New York, New York, United States

<sup>2</sup>Department of Ophthalmology, Weill Cornell Medical College, New York, New York, United States

<sup>3</sup>Department of Radiation Oncology, Memorial Sloan Kettering Cancer Center, New York, New York, United States

<sup>4</sup>Department of Pathology, Memorial Sloan Kettering Cancer Center, New York, New York, United States

<sup>5</sup>Department of Surgery (Head and Neck Service), Memorial Sloan Kettering Cancer Center, New York, New York, United States

<sup>6</sup>Department of Medicine, Memorial Sloan Kettering Cancer Center, New York, New York, United States

<sup>7</sup>Department of Medicine, Weill Cornell Medical College, New York, New York, United States

Correspondence: Jasmine H. Francis, Memorial Sloan Kettering Cancer Center, 1275 York Ave, New York, NY 10065, USA; [francij1@mskcc.org](mailto:francij1@mskcc.org).

**Received:** July 21, 2022

**Accepted:** November 15, 2022

**Published:** December 16, 2022

Citation: Francis JH, Barker CA, Brannon AR, et al. Detectability of plasma-derived circulating tumor DNA panel in patients undergoing primary treatment for uveal melanoma. *Invest Ophthalmol Vis Sci.* 2022;63(13):17. <https://doi.org/10.1167/iovs.63.13.17>

**PURPOSE.** To investigate the presence of plasma circulating tumor DNA (ctDNA) in patients with uveal melanoma during and after primary tumor treatment.

**METHODS.** Detectability and variant allele frequency of ctDNA were assessed using a 129-ogene panel using next-generation deep sequencing and hybridization capture in 69 patients with uveal melanoma undergoing primary treatment with enucleation ( $n = 8$ , during surgery) or plaque brachytherapy ( $n = 61$ ; postoperative day 0, 1, 2, or 3). Follow-up assessments were performed in 39 patients over a median of 21 months (range, 3.2–31.9 months) of follow-up. Correlations between genomic data and disease parameters were performed.

**RESULTS.** Overall, ctDNA was detectable in 20 of 69 patients with uveal melanoma (28.9%) during the perioperative period. On the day of enucleation, ctDNA was detected in two of eight patients (25%). In patients undergoing brachytherapy, ctDNA was significantly more detectable on postoperative days 2 or 3 compared with postoperative day 0 or 1 (32.4% vs 0.0%;  $P = 0.0015$ ). Patients with follow-up ctDNA that became detectable or had an increased variant allele frequency were significantly more likely to develop metastasis compared with patients with follow-up ctDNA that became undetectable or decreased variant allele frequency ( $P = 0.04$ ). In patients with detectable vs. undetectable ctDNA, there was no significant difference in tumor size, stage or location.

**CONCLUSIONS.** ctDNA is significantly more detectable at 48 to 72 hours after plaque brachytherapy compared with less than 48 hours. ctDNA can be detected during enucleation. Relative increases in ctDNA levels may herald the development of clinically apparent metastases.

**Keywords:** uveal melanoma, metastasis, circulating tumor DNA, liquid biopsy, biomarker

Although there is little published information about uveal melanoma DNA fragments in plasma (circulating tumor DNA [ctDNA]),<sup>1–5</sup> this has been studied in other solid tumors<sup>1,6,7</sup> and recently in retinoblastoma.<sup>8</sup> Before treatment, plasma ctDNA can be used for diagnosis, in differential diagnosis and molecular characterization of specific targetable mutations (e.g., *EGFR* in lung cancer).<sup>9</sup> As a result, it has replaced conventional surgical biopsy and even needle biopsy in the diagnosis of some cancers. After cancer surgery (and after temporary increases in plasma ctDNA related to surgical trauma<sup>10</sup>), plasma ctDNA promptly decreases or disappears and in those patients' subsequent detection;

increasing levels are associated with a worse prognosis.<sup>7</sup> As a result, repeated measurements are being used to monitor the effectiveness of treatment and restarting additional treatment or altering the specific targeted molecule used.<sup>6,7,11</sup> In retinoblastoma, we have recently shown that cell-free *RBI* fragments are detectable, that immediately after severing the optic nerve during surgery levels decrease (half-life of 10 minutes), or that after intra-arterial chemotherapy levels will decrease and remain at zero unless metastases develop when levels appear again.<sup>8</sup>

There have been some studies on the impact of external beam irradiation or stereotactic radiation in solid tumors

on plasma ctDNA,<sup>12–14</sup> but none in cutaneous or ocular melanoma. We recently reported that ctDNA could be detected in the plasma of untreated patients with uveal melanoma and that increasing levels detected after treatment could precede the clinical appearance of metastases.<sup>15</sup>

In the present study, we evaluate the presence of ctDNA (specifically a CLIA-approved 129-oncogene panel of somatic mutations) in plasma of patients with uveal melanoma undergoing treatment of their primary uveal melanoma. Given that ctDNA is released into blood as tumor cells undergo necrosis or apoptosis, and that plaque brachytherapy induces these two mechanisms, we hypothesized that the timing of blood draw during a 3-day plaque brachytherapy may influence the presence of ctDNA; this was a concept we also investigated along with clinical correlations and presence/levels of ctDNA in the months after primary treatment.

## METHODS

This study adhered to the tenets of the Declaration of Helsinki and was approved by the Institutional Review Board of Memorial Sloan Kettering Cancer Center. This retrospective, single-center study included 69 eligible patients from Memorial Sloan Kettering Cancer Center, New York, between February 2020 and June 2022. Informed consent was provided. Eligible patients had medium- or large-uveal melanoma (defined by Collaborative Ocular Melanoma Study criteria), absence of other known active malignancies, and had at least one ctDNA plasma specimen at the time of primary treatment with enucleation or plaque brachytherapy. Follow-up was defined from initial ctDNA to last clinical assessment (14 months for all patients and 21 months for patients with repeat ctDNA).

Clinical status was evaluated with indirect ophthalmoscopy, fundus photography, B-scan ultrasound examination or ultrasonic biomicroscopy (Ellex, Adelaide, Australia) and abdominal magnetic resonance imaging (MRI) and chest computed tomography scans. Clinical features and demographics included age, sex, and clinical status, and tumor features included largest basal diameter, height, location, laterality of disease, Collaborative Ocular Melanoma Study size, 8th edition American Joint Committee on Cancer stage, and primary treatment type (enucleation vs. plaque brachytherapy) (Table 1). Specimen data included time of collection in relation to primary treatment: enucleation (as optic nerve was severed) or plaque brachytherapy (either postoperative day 0, 1, 2, or 3: plaque brachytherapy had an apical height dose of 85 Gy over 72 hours, such that post-

operative day 0 was during placement and day 3 was during plaque removal).

ctDNA that was present during primary treatment was defined as any timepoint from day 0 to 3 (69 patients). Follow-up ctDNA were defined any timepoint more than 30 days from initial treatment (39 patients; median 21-month follow-up, range 3.2–31.9 months). Patients with initial undetectable ctDNA had specimens drawn at approximately 6-month office visits; from February 2022, patients whose most recent specimen was undetectable did not have additional specimens. All patients underwent routine radiographic surveillance, which consisted of an abdominal MRI with and without contrast every 6 months, except for patients with detectable ctDNA, who had subsequent specimens drawn (Table 2), along with an abdominal MRI approximately every 3 months and chest computed tomography scans for patients with SF3B1 mutations. There were no patients with perioperative specimens. Each specimen consisted of two 10-mL whole blood sample collected in Streck ctDNA blood collection tubes (STRECK, La Vista, NE, USA).

The MSK-ACCESS assay analyzed ctDNA plasma using deep sequencing and hybridization capture to detect very low frequency somatic alterations in exons and introns from 129 oncogenes. This includes *GNAQ* exon 5, *GNA11* exon 5, *SF3B1* exons 14, 15, 18, and *EIF1AX* exons 1 and 2. This assay was approved for clinical use by the New York State Department of Health on May 31, 2019. It can detect copy number alterations, insertions or deletions of bases and single nucleotide polymorphisms. Variant allele frequencies (VAF) are the proportion of allele bearing the variants divided by the total number of wild-type plus variant alleles at a given genomic location; at or above 0.1% were recorded. Matched white blood cell sequencing was used to both filter out germline alterations and alterations associated with clonal hematopoiesis.<sup>16</sup>

Statistical analysis used the two-tailed Student *t* test for continuous variables and Fisher's exact test for categorical variables using GraphPad software ([www.graphpad.com](http://www.graphpad.com)). For additional details on the MSK-ACCESS assay, please see the Supplementary Material.

## RESULTS

During the study, 20 patients (28.9%) had detectable plasma ctDNA. The proportion of patients with detectable vs. undetectable ctDNA during primary treatment is demonstrated in Figure 1a. Note that two of eight patients (25%) undergoing enucleation had detectable ctDNA at optic nerve severing. For plaque patients ( $n = 61$ ), ctDNA was

TABLE 1. Comparison of Patient and Tumor Data in Patients With Present vs. Absent ctDNA at Primary Treatment

	Detectable at Baseline ( $n = 13$ )	Undetectable at Baseline ( $n = 56$ )	<i>P</i> Value
Age (y)	62.5 ± 11.5	68.5 ± 12.1	0.26
Male sex	4 (31.0)	35 (62.5)	0.06
Right eye	6 (46.0)	26 (46.4)	1.00
LBD (mm)	11 ± 4.4	11.5 ± 3.4	0.71
Height (mm)	3.9 ± 3.8	4.5 ± 2.8	0.55
Ciliary body involvement	3 (23.1)	12 (21.4)	1.00
AJCC T3 or T4	5 (38.5)	19 (33.9)	0.76
COMS large	4 (30.8)	15 (26.8)	0.74
Follow-up (mo)	18.2 ± 8.5 (range, 3.3–26.1)	13.9 ± 8.3 (range 2.1–30.4)	0.64

AJCC, 8th edition American Joint Committee on Cancer; COMS, Collaborative Ocular Melanoma Study; height, ultrasound height to the tumor-scleral border; LBD, largest basal diameter.

Values are mean ± standard deviation or number (%).

TABLE 2. Details of ctDNA Alterations for Patients With Detectable Results and Subsequent ctDNA Specimens

Age and Sex	Primary tx	AJCC T	Initial ctDNA Findings	Initial ctDNA VAF	Timepoint (From Primary tx) of Subsequent Specimen and VAF	Radiographic Metastatic STATUS
Initially detectable, VAF increased						
70s F	Plaque	cT2a	TP53 exon5 p.A161V	1.29%	20 mo: 2.09%	No mets through 20 mo
80s M	Plaque	cT2a	NF1 exon26 p.N1156D	0.32%	4 mo: GNAS exon8 p.R201C 0.19%, NF1 0.43%	No mets through 16 mo
60s F	Plaque	cT2a	SF3B1 exon15 p.K700E	0.59%	1 mo: 0.43%; 5 mo: 0.54%; 8 mo: 0.60%	No mets through 8 mo
50s F	Plaque	cT1a	SF3B1 exon14 p.K666R	1.42%	5 mo: 1.59%	No mets through 5 mo
60s F	Plaque	cT3b	GNAQ exon5 p.Q209L; NF1 exon27 p.G1168D	GNAQ: 0.37%; NF1: 0.25%	8 mo: NF1 0.28%, GNAQ 0%, MSH2 exon4 p.E260K 0.64%; 20 mo: NF1 0.31%, TSC2 exon39 p.X1690_splice 0.7%	No mets through 28 mo
60s M	Enuc	cT3a	GNAQ exon5 p.Q209L; KEAP1 exon3 p.C395Y	GNAQ: 0.32%; KEAP1 0.28%	1 mo: GNAQ 0%, KEAP1 0.2%; 6 mo: GNAQ 0%, KEAP1 0.11%; 12 mo: GNAQ 0%, KEAP1 0.35%	No mets through 13 mo
70s F	Plaque	cT2b	<b>GNAS exon8 p.R201H</b>	<b>0.29%</b>	<b>7 mo: 0.53%; 13 mo: 0.53%; 19 mo: 0.72%</b>	<b>Mets at 15 mo</b>
Initially detectable, Became undetectable						
70s M	Plaque	cT4b	SF3B1 exon14 p.R625C	0.16%	1 mo: 0%	No mets through 3 mo
40s F	Plaque	cT1a	FOXO1 exon1 p.S22W	0.25%	12 mo: 0%; 18 mo: 0%; 25 mo: 0%	No mets through 24 mo
60s F	Plaque	cT2a	CDKN2A exon2 p.D108N	0.13%	9 mo: 0%; 15 mo: 0%	No mets through 23 mo
50s F	Plaque	cT3b	GNA11 exon5 p.Q209L; SF3B1 exon14 p.R625H	GNAQ 1.22%; SF3B1 1.27%	7 mo: 0%; 13 mo: 0%; 19 mo: 0%	No mets through 26 mo
50s F	Plaque	cT2b	GNAQ exon5 p.Q209L; EIF1AX exon2 p.R13P	GNAQ 0.88%; EIF1AX 0.56%	1 mo: 0%	No mets at 1 mo
Initially detectable, no follow-up						
40s M	Enuc	cT3b	FOXO1 exon1 p.S22W	1.26%	No f/u	No f/u
Initially undetectable, became detectable						
60s M	Plaque	cT2a	N/A	N/A	8 mo: TRK1-FRRS1 rearrangement: c.1838:NTRK1_c.1120+62:FRRS1inv; 17 mo: undetectable	No mets through 17 mo
50s M	Plaque	cT2a	N/A	N/A	0.1 mo: 0%; 12 mo: 0%; 18 mo: SF3B1 exon14 p.K666Q 1.65%	No mets through 25 mo
50s M	Plaque	cT2a	N/A	N/A	8 mo: MSH6 exon2 p.L148I 0.22%	no mets through 8 mo
70s M	Plaque	cT3a	N/A	N/A	20 mo: TP53 exon7 p.R248Q 0.48%, ATM exon50 p.V2441D 0.64%	No mets through 24 mo
60s F	Plaque	cT2a	N/A	N/A	<b>12 mo: FOXO1 exon1 p.S22W 0.6%; 19 mo: 0.91%</b>	<b>Mets at 20 mo</b>
60s F	Plaque	cT2a	N/A	N/A	8 mo: 0%; 14 mo: NF1 exon47 p.D2326Y 0.32%	No mets through 18 mo
50s F	Plaque	cT2c	N/A	N/A	<b>5 mo: ATM exon4 p.S99G 0.4%; SF3B1 exon16 p.R775G 15.49%; 8 mo: ATM 0.16%, SF3B1 11.05%; 9 mo: ATM 0.37%, SF3B1 6.11%; 11 mo: ATR 4.7%, SF3B1 5.2%</b>	<b>Mets at 18 mo</b>

AJCC, American Joint Committee on Cancer; ctDNA, circulating tumor DNA; enuc, enucleation; mets, metastasis; tx, treatment; VAF, variant allele frequency.

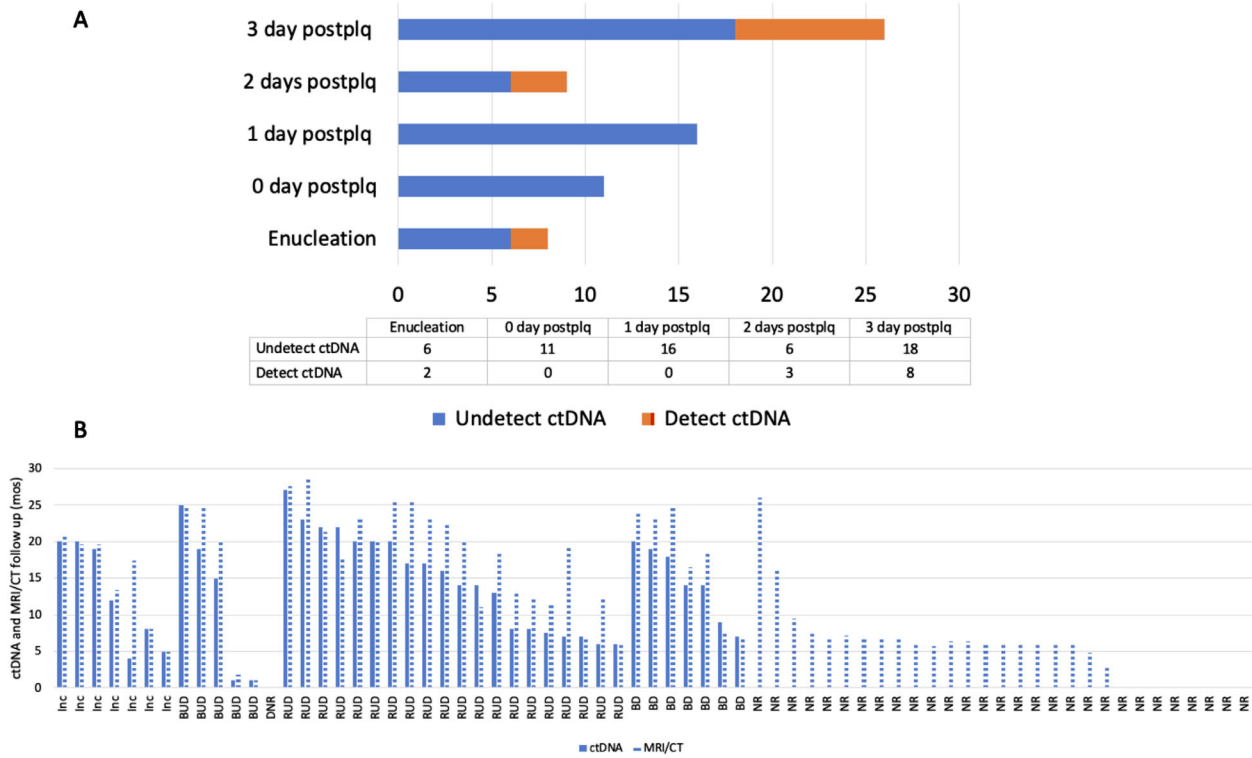


**FIGURE 1.** (A) Box plot showing proportion of patients with detectable vs. undetectable ctDNA during primary treatment. ctDNA, circulating tumor DNA; detect, detectable; Postplq, postplaque brachytherapy; undetect, undetectable. (B) Column graph demonstrating follow-up months for repeat ctDNA and radiographic surveillance. BD, initially undetectable became detectable; BUD, initially detectable and became undetectable; CT, computed tomography; ctDNA, circulating tumor DNA; DNR, initially detectable no repeat ctDNA; Inc, initially detectable and VAF increased over follow-up; MRI, magnetic resonance imaging; NR, initially undetectable no repeat ctDNA; RUD, initially undetectable remained undetectable.

significantly more likely to be detected on postoperative day 2 or 3 compared with during plaque insertion or day 1 (32.4% vs. 0.0%;  $P = 0.0015$ ). Figure 1b demonstrates follow-up time for ctDNA and radiographic studies per patient. The median follow-up was 21 months (range, 3.2–31.9 months). Table 1 compares patient and tumor data of

patients with present vs. absent ctDNA at primary treatment. There was no statistical difference between the groups, including tumor size, stage, and location.

Figure 2 is a flow diagram depicting the subsequent ctDNA results and correlation with metastatic status. Of 13 patients with ctDNA present at primary treatment, 5 had

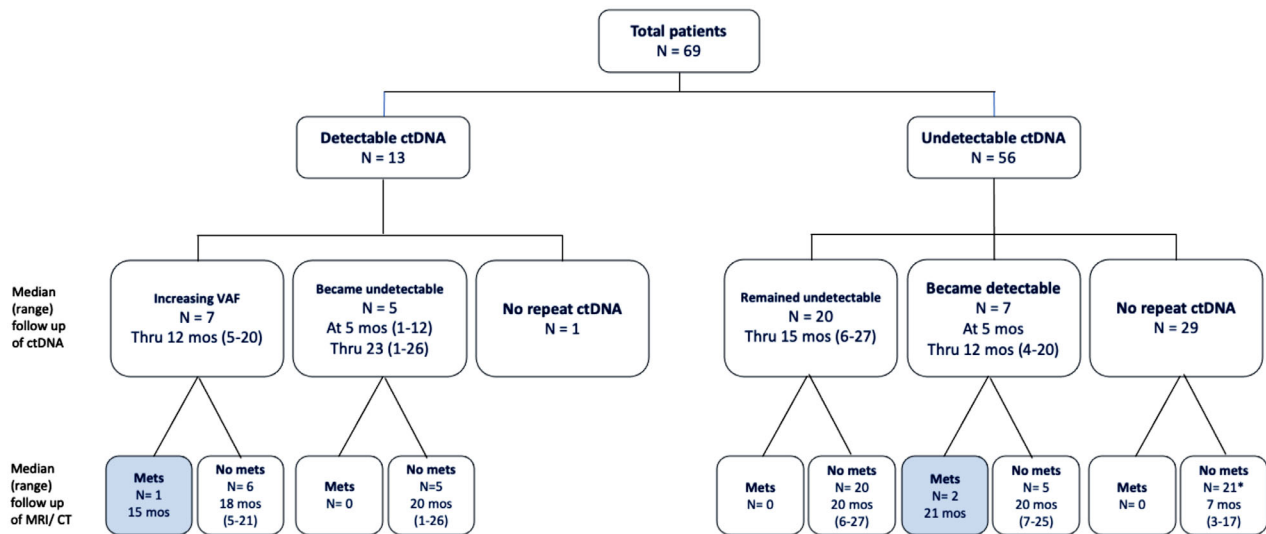


**FIGURE 2.** Flow diagram depicting the subsequent ctDNA results and correlation with metastatic status. Each box lists the clinical status on the first line, the number of patients on the second line and, if applicable, the median time of follow-up or median time of event (became undetectable or detectable) on the third line and range in parentheses. The clinical status of metastatic disease was determined by date of radiographic metastasis which were subsequently biopsy confirmed. ctDNA, circulating tumor DNA; mets, metastasis; MRI/CT, magnetic resonance imaging/computed tomography; VAF, variant allele frequency. \*Of 30 patients without repeat ctDNA specimen, 21 patients continued to receive radiographic surveillance.

subsequent undetectable ctDNA and 7 had increasing VAF. Of patients with initial undetectable ctDNA, 7 (of 39 patients with repeat testing) had the presence of plasma ctDNA on subsequent testing at a median 12 months after primary treatment. Three patients developed metastatic disease: one patient with increasing VAF after primary treatment and two patients who developed detectable ctDNA after undetectability at primary treatment. No patient with ctDNA that became or remained undetectable had radiographic metastasis. By Fisher's exact test, patients with follow-up ctDNA that became detectable or increased VAF were significantly more likely to develop metastasis compared with patients with follow-up ctDNA that became undetectable or decreased VAF ( $P = 0.04$ ).

Table 2 outlines patients with detectable ctDNA somatic alterations, detailing the specific alteration, VAF, and subsequent timepoints and their ctDNA results along with radiographic metastatic status. Neither patient who developed metastatic disease had typical mutations known to initiate or drive uveal melanoma: one had *GNAS* exon8 p.R201H and the other *FOXO1* exon1 p.S22W; both had a VAF trending higher over time before radiographic metastasis.

## DISCUSSION

Our study demonstrates that oncogene-associated somatic ctDNA can be detected in the plasma of a minority of patients with uveal melanoma undergoing primary treatment. The presence of plasma ctDNA seems to be associated with the timing of the blood specimen retrieval for patients receiving brachytherapy for their primary tumor. For patients undergoing 3-day plaque brachytherapy, ctDNA was present only on postoperative days 2 and 3, but not on postoperative day 0 or 1. Because ctDNA is released into the blood by necrotic and apoptotic tumor cells, this finding may suggest plaque brachytherapy induces these cell death mechanisms within 24 to 48 hours of starting tumor irradiation. In lung cancer, stereotactic radiation increases plasma ctDNA (levels increase after 24 hours and peak at 7 days)<sup>13</sup>; a similar postirradiation increase in plasma ctDNA has been shown in preclinical models of head and neck cancer.<sup>14</sup> No published study has demonstrated these trends with brachytherapy; however, our results suggest that brachytherapy increases plasma ctDNA in uveal melanoma. Serial measurements during plaque brachytherapy on the same patient would be particularly useful at confirming this hypothesis and this is a future endeavor of ours and other investigators.

One study used aqueous humor-derived ctDNA to detect copy number alterations before and after radiation for uveal melanoma.<sup>17</sup> None of the choroidal melanomas had detectable ctDNA at any timepoint, and six of the eight ciliary body tumors had ctDNA only after radiation.<sup>17</sup> Although this study did not specify the postirradiation timepoint, it suggests, like our findings, that radiation allows for the release of tumor DNA into bodily fluids so that it may be detectable by aqueous humor and plasma liquid biopsy. Furthermore, Im et al.<sup>17</sup> showed that tumor location was a significant factor in ctDNA detectability (only ciliary body tumors had ctDNA present). Bustamante et al.<sup>4</sup> found a relationship between levels of droplet PCR-based ctDNA (of four genes) and 8th edition American Joint Committee on Cancer classification and tumor thickness. In contrast, our study found no significant difference in ctDNA detectability based on tumor size, stage, or location. These data warrant confir-

mation by larger studies, but they may suggest that aqueous humor-based assays are influenced by tumor location, whereas serum-based assays are not.

Even though detecting metastatic disease was not the initial intention of this study, nor was the methodology formalized to explore ctDNA as it relates to metastatic disease status, there are a few observations to be made. In our relatively short-term median follow-up of 21 months, no patient with ctDNA that became or remained undetectable had radiographic metastasis. The three patients with metastatic disease that developed over the study duration all had detectable ctDNA in plasma: one had *GNAS* R201H present at primary treatment, one developed detectable *SF3B1* p.R775G & *ATM* p.S99G 5-month after primary treatment and the last developed detectable *FOXO1* S22F ctDNA at 12 months after primary treatment. No patient had radiographically evident metastasis at initial ctDNA presence, and the time to metastasis was 8, 18, and 7 months, respectively. For all three patients, ctDNA preceded radiographic metastasis and was trending upward over serial measurements. To this point, patients with follow-up ctDNA that became detectable or increased VAF were significantly more likely to develop metastasis compared with patients with follow-up ctDNA that became undetectable or decreased VAF. This finding may suggest that a relative increase in ctDNA VAF is a biomarker for metastatic disease and could offer two clinical translations for uveal melanoma management: first, that detectable ctDNA could be monitored with serial measurements; and second, that relative VAF increases may prompt a shorter interval between systemic surveillance, or potentially initiating metastasis directed therapy before the development of clinically or radiographically apparent metastasis.

Up until recently, the dearth of effective treatment for metastatic uveal melanoma meant that, lead-time bias aside, earlier detection of systemic disease did not offer improved outcome. However, with US Food and Drug Administration approval of tebentafusp earlier this year, patients with uveal melanoma and an HLA-A 02:01 allele now have an option that improves median overall survival.<sup>18</sup> Clinical trials of this bispecific fusion protein-based immunotherapy suggest that an earlier detection of metastatic disease may result in better overall survival.<sup>18</sup> Consequently, there is now motivation for earlier metastatic disease detection and plasma ctDNA may offer an advantage over standard radiographic surveillance, as shown here and in our other work.<sup>15</sup>

The advantage of the multigene panel is the ability to test for 129 different oncogenes. Four of these genes are believed to play a role in uveal melanoma: the initiating genes *GNAQ* and *GNA11* and driving genes *EIF1AX* and *SF3B1*. Unlike other studies that are restricted to hotspot mutations on a few relevant genes,<sup>2-4,19,20</sup> our next-generation sequencing platform looks at the exons of these four genes in addition to an additional 125 oncogenes. Perhaps owing to its size, there are no published plasma-based ctDNA assays looking at *BAP1* in uveal melanoma (only one report of *BAP1* in aqueous humor-derived ctDNA<sup>17</sup>), and owing to constraints imposed by the coronavirus disease 2019 pandemic, the inclusion of *BAP1* in our assay did not come to fruition for the present study. However, we are anticipating the addition of this gene in an upcoming version of the assay.

Interestingly, detectable ctDNA in our uveal melanoma cohort was not excluded to *GNAQ*, *GNA11*, *EIF1AX* and *SF3B1*. Ten other genes were detected and consisted of *NF1*

(three patients), *TP53* (two patients), *GNAS* (two patients), *ATM* (two patients), *FOXO1* (three patients), *MSH2*, *MSH6*, *TSC2*, *KEAP1*, and *CDKN2A*. Furthermore, the only three patients who developed metastatic disease exhibited two of these alternate genes: *GNAS* exon8 p.R210H, *ATM* S99G, and *FOXO1* exon1 p.S22W. Without confirmatory sequencing data from the solid tumor, it was not possible to confirm that origins of the specific mutations found on liquid biopsy ctDNA.

However, the correlation between increasing levels of these genes in coordination with the development and progression of metastatic disease would suggest these genes were markers of uveal melanoma metastasis, albeit in three patients. Across the study, three patients had detectable *FOXO1* S22F alterations and two had *GNAS* R201H alterations, suggesting that these genes may be recurrent events that may play a previously underexplored role in uveal melanoma development. Further studies of ctDNA in patients with high-risk primary uveal melanoma or metastatic uveal melanoma should include genes such as *GNAS* and *FOXO1*, not just uveal melanoma-associated genes like *GNAQ* and *GNA11*, in panels to help elucidate how these genes play a role in development of metastases. Other explanations for these alternate genes are the presence of other malignancies, although we excluded patients with other active malignancies to avoid this confounder. They are unlikely to represent clonal hematopoiesis or germline alterations because the assay methodology screens these mutations out. We do not understand why the patients with metastases and detectable ctDNA did not all have *GNAQ/GNA11* mutations, and we hope more follow-up will help elucidate this.

This study is limited by its retrospective nature, lack of serial perioperative measurements, and inconsistent schedule of specimen collection and metastatic surveillance. However, we believe it offers useful information to help guide the design of future studies on ctDNA in uveal melanoma. First, we show that the timing of plasma collection during plaque brachytherapy will likely influence rates of ctDNA detection, with a notable higher rate of detection at 2- and 3-day postradiation specimens compared with earlier collections. Second, ctDNA from genes such as *GNAS* and *FOXO1* were found in multiple patients, including those who developed metastatic disease, suggesting ctDNA panels should expand beyond the several genes typically considered associated with uveal melanoma. And finally, presence of upward trending ctDNA levels may herald metastatic disease and may warrant adjustments in surveillance schedule and guide future clinical trial development. We look forward to future studies to help answer these questions.

### Acknowledgments

Supported by philanthropic funding from The Macula Society [JHF], The Fund for Ophthalmic Knowledge [JHF, DHA] and the Cancer Center Support Grant (P30 CA008748). All authors report grant from National Institutes of Health, during the conduct of the study. The sponsor or funding organization had no role in the design or conduct of this research.

Disclosure: **J.H. Francis**, None; **C.A. Barker**, grants from Merck, grants from Amgen, personal fees and non-financial support from American Society for Radiation Oncology, personal fees and non-financial support from American Brachytherapy Society, non-financial support from National Comprehensive Cancer Network outside the submitted work; **A.R. Brannon**, None;

**J. Canestraro**, None; **M. Robbins**, None; **C.E. Swartzwelder**, None; **S. Levine**, None; **C. Law**, None; **M.F. Berger**, Grail, Roche, patent; **A. Shoushtari**, Consulting fees from BMS, Immunocore, and Novartis, research support to my institution from Bristol-Myers Squibb, Immunocore, Novartis, Polaris, Pfizer, Checkmate Pharmaceuticals, Foghorn Therapeutics, Linnaeus Therapeutics, Targovax; **D.H. Abramson**, None

### References

- Bettegowda C, Sausen M, Leary RJ, et al. Detection of circulating tumor DNA in early- and late-stage human malignancies. *Sci Transl Med.* 2014;6(224):224ra24–224ra24, doi:10.1126/scitranslmed.3007094.
- Bidard F-C, Madic J, Mariani P, et al. Detection rate and prognostic value of circulating tumor cells and circulating tumor DNA in metastatic uveal melanoma. *Int J Cancer.* 2014;134(5):1207–1213, doi:10.1002/ijc.28436.
- Metz CH, Scheulen M, Bornfeld N, Lohmann D, Zeschnigk M. Ultradeep sequencing detects GNAQ and GNA11 mutations in cell-free DNA from plasma of patients with uveal melanoma. *Cancer Med.* 2013;2(2):208–215, doi:10.1002/cam4.61.
- Bustamante P, Tsering T, Coblentz J, et al. Circulating tumor DNA tracking through driver mutations as a liquid biopsy-based biomarker for uveal melanoma. *J Exp Clin Cancer Res.* 2021;40(1):196, doi:10.1186/s13046-021-01984-w.
- Fiala C, Diamandis EP. Cell-free DNA analysis in cancer. *N Engl J Med.* 2019;380(5):501, doi:10.1056/NEJMc1816154.
- Murtaza M, Dawson S-J, Tsui DWY, et al. Non-invasive analysis of acquired resistance to cancer therapy by sequencing of plasma DNA. *Nature.* 2013;497(7447):108–112, doi:10.1038/nature12065.
- Diaz LA, Bardelli A. Liquid biopsies: genotyping circulating tumor DNA. *J Clin Oncol.* 2014;32(6):579–586, doi:10.1200/JCO.2012.45.2011.
- Francis JH, Gobin YP, Brannon AR, et al. RB1 circulating tumor DNA in the blood of patients with unilateral retinoblastoma: before and after intra-arterial chemotherapy. *Ophthalmol Sci.* 2021;1(3):100042, doi:10.1016/j.xops.2021.100042.
- Mack PC, Miao J, Redman MW, et al. Circulating tumor DNA (ctDNA) kinetics predict progression-free and overall survival in EGFR TKI-treated patients with EGFR-mutant NSCLC (SWOG S1403). *Clin Cancer Res.* 2022;28(17):3752–3760, doi:10.1158/1078-0432.CCR-22-0741.
- Henriksen TV, Reinert T, Christensen E, et al. The effect of surgical trauma on circulating free DNA levels in cancer patients-implications for studies of circulating tumor DNA. *Mol Oncol.* 2020;14(8):1670–1679, doi:10.1002/1878-0261.12729.
- Dawson S-J, Tsui DWY, Murtaza M, et al. Analysis of circulating tumor DNA to monitor metastatic breast cancer. *N Engl J Med.* 2013;368(13):1199–1209, doi:10.1056/NEJMoa1213261.
- Corradetti MN, Torok JA, Hatch AJ, et al. Dynamic changes in circulating tumor DNA during chemoradiation for locally advanced lung cancer. *Adv Radiat Oncol.* 2019;4(4):748–752, doi:10.1016/j.adro.2019.05.004.
- Kageyama S-I, Nihei K, Karasawa K, et al. Radiotherapy increases plasma levels of tumoral cell-free DNA in non-small cell lung cancer patients. *Oncotarget.* 2018;9(27):19368–19378, doi:10.18632/oncotarget.25053.
- Muhanna N, Eu D, Chan HHL, et al. Cell-free DNA and circulating tumor cell kinetics in a pre-clinical head and neck cancer model undergoing radiation therapy. *BMC Cancer.* 2021;21(1):1075, doi:10.1186/s12885-021-08791-8.
- Francis JH, Canestraro J, Brannon AR, et al. Association of plasma circulating tumor DNA with diagnosis of metastatic

- veal melanoma. *JAMA Ophthalmol.* 2021;139(11):124–1245, doi:[10.1001/jamaophthalmol.2021.3708](https://doi.org/10.1001/jamaophthalmol.2021.3708).
16. Rose Brannon A, Jayakumaran G, Diosdado M, et al. Enhanced specificity of clinical high-sensitivity tumor mutation profiling in cell-free DNA via paired normal sequencing using MSK-ACCESS. *Nat Commun.* 2021;12(1):3770, doi:[10.1038/s41467-021-24109-5](https://doi.org/10.1038/s41467-021-24109-5).
17. Im DH, Peng C-C, Xu L, et al. Potential of aqueous humor as a liquid biopsy for uveal melanoma. *Int J Mol Sci.* 2022;23(11):6226, doi:[10.3390/ijms23116226](https://doi.org/10.3390/ijms23116226).
18. Nathan P, Hassel JC, Rutkowski P, et al. Overall survival benefit with tebentafusp in metastatic uveal melanoma. *N Engl J Med.* 2021;385(13):1196–1206, doi:[10.1056/NEJMoa2103485](https://doi.org/10.1056/NEJMoa2103485).
19. Beasley A, Isaacs T, Khattak MA, et al. Clinical application of circulating tumor cells and circulating tumor DNA in uveal melanoma. *JCO Precis Oncol.* 2018;2:PO.17.00279, doi:[10.1200/PO.17.00279](https://doi.org/10.1200/PO.17.00279).
20. Madic J, Piperno-Neumann S, Servois V, et al. Pyrophosphorolysis-activated polymerization detects circulating tumor DNA in metastatic uveal melanoma. *Clin Cancer Res.* 2012;18(14):3934–3941, doi:[10.1158/1078-0432.CCR-12-0309](https://doi.org/10.1158/1078-0432.CCR-12-0309).